Strategies for the Assembly of Homo- and Hetero-nuclear Metallosupramolecules containing 2,2′:6′,2″-Terpyridine Metal-binding Domains†

Edwin C. Constable* and Alexander M. W. Cargill Thompson
Institut für Anorganische Chemie, Spitalstrasse 51, CH-4056 Basel, Switzerland

A new strategy for the convergent synthesis of metallosupramolecular oligomers has been elaborated. The key step is the formation of the *ligand-complexes* $[Ru(X\text{-}terpy)(dpqtpy)][PF_6]_2$ (X-terpy = terpy, eoterpy, cterpy or msterpy) from the reaction of $[Ru(X\text{-}terpy)Cl_3]$ with 6′,6″-di(2-pyridyl)-2,2′:4′,4″:2″,2‴-quaterpyridine (dpqtpy) in ethane-1,2-diol. These complexes have one non-co-ordinated terpyridine (terpy) domain, and reacted instantaneously with iron(II) salts to give the heterotrinuclear complexes $[(X\text{-}terpy)Ru(dpqtpy)Fe(dpqtpy)Ru(X\text{-}terpy)][PF_6]_6$. Similar reactions with cobalt(II) acetate gave the paramagnetic d^7 cobalt(II) complexes $[(X\text{-}terpy)Ru(dpqtpy)Co(dpqtpy)Ru(X\text{-}terpy)][PF_6]_6$ which may be oxidised to the kinetically inert diamagnetic d^6 cobalt(III) complexes $[(X\text{-}terpy)Ru(dpqtpy)Co(dpqtpy)Ru(X\text{-}terpy)][PF_6]_7$. The reaction of $[Ru(X\text{-}terpy)(dpqtpy)][PF_6]_2$ with '$RuCl_3 \cdot nH_2O$' yielded the homotrinuclear complex $[(terpy)Ru(dpqtpy)Ru(dpqtpy)Ru(terpy)][PF_6]_6$. The ruthenium–osmium heterodinuclear complex $[(terpy)Ru(dpqtpy)Os(terpy)][PF_6]_4$ was readily obtained from the reaction of $[Ru(terpy)(dpqtpy)][PF_6]_2$ with $[Os(terpy)Cl_3]$. Some representative mixed-ligand homodinuclear complexes $[(X\text{-}terpy)Ru(dpqtpy)Ru(Y\text{-}terpy)][PF_6]_4$ containing both electron-releasing and electron-withdrawing terminator ligands were prepared from the reaction of $[Ru(X\text{-}terpy)(dpqtpy)][PF_6]_2$ with an equimolar quantity of $[Ru(Y\text{-}terpy)Cl_3]$. The specific examples with mixed terminator ligands were $[(terpy)Ru(dpqtpy)Ru(dmterpy)][PF_6]_4$, $[(terpy)Ru(dpqtpy)Ru(msterpy)][PF_6]_4$ and $[(dmterpy)Ru(dpqtpy)Ru(msterpy)][PF_6]_4$. All of the compounds were fully characterised, and detailed spectroscopic, spectrometric and electrochemical studies are described.

Metallosupramolecular oligomers and polymers result from the interaction of metal ions with appropriate multidentate ligands designed for multinuclear binding,[1–3] and there is considerable interest in the design of species containing known numbers of metal ions in defined spatial arrangements.[4] The electronic and photophysical properties of oligopyridine complexes of d^6 transition-metal ions make their incorporation particularly attractive and the possibility of intermetallic electron or energy transfers offers the potential for the design of molecular devices which will channel light energy or electrons in a defined manner.[5]

We have discussed elsewhere the reasons which have led us and others to adopt the 2,2′:6′,2″-terpyridine (terpy) metal-binding domain and have developed a strategy for the stepwise self-assembly of metallosupramolecules utilising multidentate ligands which contain two or more spatially separated terpy metal-binding domains.[1,6] The preparation and properties of some iron(II)[7] and ruthenium(II)[8,9] complexes have been reported, as have studies on related heteronuclear ruthenium–osmium complexes.[10] However, the preparation of high-nuclearity complexes using a divergent complexes-as-metals approach is problematic. It becomes increasingly difficult specifically to address only one of the metal-binding domains in a multidomain ligand. An *organic* protection–deprotection methodology has recently been introduced to overcome this problem, but this involves a multistep reaction sequence.[11] In this paper we describe a method for the convergent synthesis of asymmetric dinuclear complexes and an alternative *inorganic* methodology for the stepwise assembly of co-ordination oligomers making use of the different rates of reactions of kinetically labile and non-labile metal centres. Some of these results have appeared in part as communications elsewhere.[12]

† Ligand abbreviations: dpqtpy = 6′,6″-di(2-pyridyl)-2,2′:4′,4″:2″,2‴-quaterpyridine; bteb = 1,4-bis(2,2′:6′,2″-terpyridin-4′-yl)benzene; terpy = 2,2′:6′,2″-terpyridine; eoterpy = 4′-ethoxy, moterpy = 4′-methoxy, dmterpy = 4′-dimethylamino, cterpy = 4′-chloro, msterpy = 4′-methylsulfonyl, mtterpy = 4′-methylsulfanyl, pterpy = 4′-phenyl, hterpy = 4′-hydroxy, pyterpy = 4′-(4-pyridyl), mpyterpy = 4′-(4-methylpyridinio) and fterpy = 4′-(ferrocenyl)-2,2′:6′,2″-terpyridine; tppz = 2,3,5,6-tetra(2-pyridyl)pyrazine.

Experimental

Proton NMR spectra were recorded on Bruker WM-250, AC-250 or Varian Gemini 300 spectrometers, electronic spectra on Uvikon 810P or Perkin-Elmer Lambda 19 spectrophotometers. Fast atom bombardment (FAB), fast ion bombardment (FIB) and laser desorption time-of-flight (LD) mass spectra were recorded on Kratos MS-890 (FAB), MS-50 (FIB), Kompact Maldi (LD) or Vestec benchtop (LD) spectrometers respectively; for FAB and FIB spectra the sample was loaded using acetonitrile as solvent, and 3-nitrobenzyl alcohol as supporting matrix; for LD spectra, the sample was dissolved in acetone or acetonitrile, and run using sinapinic acid, gentisic acid or α-cyano-4-hydroxycinnamic acid as supporting matrix. Cyclic voltammetry experiments were performed in acetonitrile solution as described previously.[7–9] All potentials are quoted against an internal ferrocene–ferrocenium reference.

Ruthenium trichloride was used as supplied by Johnson Matthey. The compounds dpqtpy,[8] terpy,[13] eoterpy,[14] dmterpy,[14] cterpy,[8,14] and msterpy[15] were prepared by the literature methods; the complexes $[Ru(X\text{-}terpy)Cl_3]$ (X-

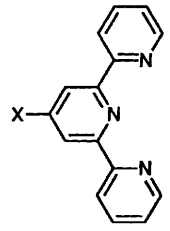

X

terpy	H
eoterpy	EtO
moterpy	MeO
dmterpy	Me_2N
cterpy	Cl
msterpy	MeO_2S
mtterpy	MeS
hterpy	HO
pterpy	Ph
fterpy	$(C_5H_4)Fe(C_5H_5)$

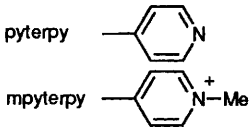

pyterpy

mpyterpy

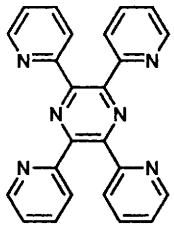

tppz

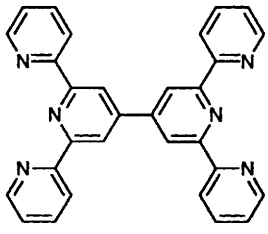

dpqtpy

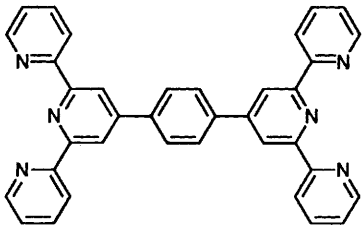

bteb

terpy = terpy, eoterpy, dmterpy, cterpy or msterpy)[14,15] were prepared as previously reported.

Preparations.—General method for [Ru^{II}(X-terpy)(dpqtpy)][PF_6]$_2$ (X-terpy = terpy, eoterpy, cterpy *or* msterpy). A suspension of dpqtpy (0.10 mmol) and [Ru(X-terpy)Cl_3] (0.09 mmol) was heated at reflux in ethane-1,2-diol (10 cm^3) for 20 min. The resulting deep red solution was allowed to cool, and then water (10 cm^3) and an excess of methanolic [NH_4][PF_6] were added to give a red precipitate. This was collected on a bed of Celite by filtration, and then redissolved in the minimum volume of MeCN and chromatographed over silica MeCN–saturated aqueous KNO_3–water (7:1:0.5 v/v) as eluent]. The main orange fraction was collected and treated with water (25 cm^3) and an excess of methanolic [NH_4][PF_6]. This mixture was then reduced in volume *in vacuo* to precipitate the desired complex as the hexafluorophosphate salt. Recrystallisation from acetone–methanol or acetonitrile–water gave the complexes as analytically pure red powders in 20–40% yields.

[Ru(dmterpy)(dpqtpy)][PF_6]$_2$. The complex [Ru(cterpy)(dpqtpy)][PF_6]$_2$ (0.100 g, 0.089 mmol) was stirred in anhydrous dimethylamine (20 cm^3) at 0 °C for 3 h. The excess of dimethylamine was then removed *in vacuo*. The residue was recrystallised from acetone–methanol to give [Ru(dmterpy)(dpqtpy)][PF_6]$_2$ as a red powder (0.094 g, 93%).

General method for the iron(II)*diruthenium*(II) *complexes* [(X-terpy)Ru(dpqtpy)Fe(dpqtpy)Ru(X-terpy)][PF_6]$_6$ (X-terpy = terpy, eoterpy, dmterpy, cterpy *or* msterpy). A solution of [$Fe(H_2O)_6$][BF_4]$_2$ (0.010 g, 0.030 mmol) in water (10 cm^3) was added to a solution of [Ru(X-terpy)(dpqtpy)][PF_6]$_2$ (0.040 mmol) in MeCN (20 cm^3) and the resulting mixture stirred at ambient temperature for 15 min. An excess of methanolic [NH_4][PF_6] was then added, and precipitation was induced by reduction in volume *in vacuo*. Recrystallisation from acetone–methanol afforded the pure salts [(X-terpy)Ru(dpqtpy)Fe(dpqtpy)Ru(X-terpy)][PF_6]$_6$ as dark red-brown powders in 70–90% yield.

[(terpy)Ru(dpqtpy)Co(dpqtpy)Ru(terpy)][PF_6]$_6$. A solution of $Co(O_2CMe)_2{\cdot}4H_2O$ (0.018 g, 0.072 mmol) in water (20 cm^3) was added to a solution of [Ru(terpy)(dpqtpy)][PF_6]$_2$ (0.040 g, 0.037 mmol) in MeCN (5 cm^3), and the resulting mixture was stirred at ambient temperature for 30 min. An excess of methanolic [NH_4][PF_6] was added, and precipitation was induced by reduction in volume *in vacuo*. Recrystallisation from acetone–methanol afforded pure [(terpy)Ru(dpqtpy)Co(dpqtpy)Ru(terpy)][PF_6]$_6$ as a brown powder (0.039 g, 84%). Mass spectrum (FIB, ^{102}Ru): *m/z* 943 [Ru(terpy)(dpqtpy)(PF_6)] and 798 [Ru(terpy)(dpqtpy)].

[(terpy)Ru(dpqtpy)Co(dpqtpy)Ru(terpy)][PF_6]$_7$. A solution of $Co(O_2CMe)_2{\cdot}4H_2O$ (0.018 g, 0.072 mmol) in water (20 cm^3) was added to a solution of [Ru(terpy)(dpqtpy)][PF_6]$_2$ (0.040 g, 0.037 mmol) in MeCN (5 cm^3), and the resulting mixture was stirred at ambient temperature for 15 min, while chlorine gas was gently bubbled through it. An excess of methanolic [NH_4][PF_6] was added, and precipitation was induced by reduction in volume *in vacuo*. Recrystallisation from acetone–methanol afforded [(terpy)Ru(dpqtpy)Co(dpqtpy)Ru(terpy)][PF_6]$_7$ as a pink-brown powder (0.047 g, 95%). Mass spectrum (FIB, ^{102}Ru): *m/z* 944 [Ru(terpy)(dpqtpy)(PF_6)] and 798 [Ru(terpy)(dpqtpy)].

[(terpy)Ru(dpqtpy)Ru(dpqtpy)Ru(terpy)][PF_6]$_6$. Two equivalents of [Ru(terpy)(dpqtpy)][PF_6]$_2$ (0.040 g, 0.037 mmol) were heated at reflux with $RuCl_3{\cdot}3H_2O$ (0.005 g, 0.019 mmol) in ethane-1,2-diol (10 cm^3) for 1.5 h. The reaction mixture was allowed to cool, and acetone (25 cm^3) and diethyl ether (25 cm^3) were added. The resulting precipitate was collected on Celite, and washed off with methanol (25 cm^3). The complex was reprecipitated from the methanol solution as the hexafluorophosphate salt by dropwise addition of [NH_4][PF_6]. Recrystallisation from acetonitrile-water afforded [(terpy)Ru(dpqtpy)Ru(dpqtpy)Ru(terpy)][PF_6]$_6$ as a dark brown powder (0.020 g, 42%). Mass spectrum (FIB, ^{102}Ru): *m/z* 2427 [(terpy)Ru(dpqtpy)Ru(dpqtpy)Ru(terpy)(PF_6)$_5$], 2281 [(terpy)Ru(dpqtpy)Ru(dpqtpy)Ru(terpy)(PF_6)$_4$] and 2135 [(terpy)Ru(dpqtpy)Ru(dpqtpy)Ru(terpy)(PF_6)$_3$].

[Os(terpy)Cl_3]. A solution of $Na_2[OsCl_6]$ (0.100 g, 0.22 mmol) and 2,2′:6′,2″-terpyridine (0.052 g, 0.22 mmol) in methanol (20 cm^3) was heated to reflux for 20 h. The resulting precipitate was filtered off, washed well with methanol and diethyl ether, and dried *in vacuo* to yield [Os(terpy)Cl_3] as a black powder (0.085 g, 72%).

[(terpy)Ru(dpqtpy)Os(terpy)][PF_6]$_4$. A suspension of [Ru(terpy)(dpqtpy)][PF_6]$_2$ (0.041 g, 0.038 mmol) and [Os(terpy)Cl_3] (0.020 g, 0.038 mmol) in ethane-1,2-diol (10 cm^3) was heated at reflux for 2 h. The resulting purple-brown

solution was allowed to cool. An equal volume of water was added, along with an excess of methanolic $[NH_4][PF_6]$, to precipitate the complex mixture. This was collected on Celite by filtration, and redissolved in the minimum volume of MeCN for thin-layer chromatography [silica plates, MeCN–saturated aqueous KNO_3–water (7:1:0.5 v/v) as eluent]. The main purple product was collected, and the complex was extracted from the silica by washing alternately with the eluent mixture and aqueous acetonitrile (1:1 v/v) acidified slightly with HPF_6. These extracts were combined and an excess of methanolic $[NH_4][PF_6]$ was added. The mixture was reduced in volume *in vacuo* to precipitate the complex as the hexafluorophosphate salt. Recrystallisation from acetonitrile–water gave [(terpy)Ru(dpqtpy)Os(terpy)][PF_6]$_4$ as a dark brown powder (0.020 g, 29%). Mass spectrum (FIB, ^{192}Os): *m/z* 1656 [(terpy)Ru(dpqtpy)Os(terpy)(PF_6)$_3$], 1512 [(terpy)Ru(dpqtpy)Os(terpy)(PF_6)$_2$] and 1367 [(terpy)Ru(dpqtpy)Os(terpy)(PF_6)].

[(terpy)Os(dpqtpy)Os(terpy)][PF_6]$_4$. A suspension of dpqtpy (0.020 g, 0.043 mmol) and [Os(terpy)Cl_3] (0.050 g, 0.095 mmol) in ethane-1,2-diol (10 cm^3) was heated at reflux for 2 h. The resulting purple-brown solution was allowed to cool. An identical work-up and purification process to that for [(terpy)Ru(dpqtpy)Os(terpy)][PF_6]$_4$ was used. After recrystallisation from acetonitrile–water, [(terpy)Os(dpqtpy)Os(terpy)][PF_6]$_4$ was obtained as a dark purple powder (0.013 g, 16%). Mass spectrum (FIB, ^{192}Os): *m/z* 1746 [(terpy)Os(dpqtpy)Os(terpy)(PF_6)$_3$], 1601 [(terpy)Os(dpqtpy)Os(terpy)(PF_6)$_2$] and 1457 [(terpy)Os(dpqtpy)Os(terpy)(PF_6)].

[Os(terpy)$_2$][PF_6]$_2$. A suspension of [Os(terpy)Cl_3] (0.040 g, 0.076 mmol) and 2,2′:6′,2″-terpyridine (0.018 g, 0.076 mmol) in ethane-1,2-diol (10 cm^3) was heated at reflux for 20 h. The resulting purple-brown solution was allowed to cool. An equal volume of water was added, along with an excess of methanolic $[NH_4][PF_6]$, to precipitate the complex mixture. This was collected on Celite by filtration, and redissolved in the minimum volume of MeCN for column chromatography [silica, MeCN–saturated aqueous KNO_3–water (7:1:0.5 v/v) as eluent]. The main brown product fraction was collected, and water (25 cm^3) and an excess of methanolic $[NH_4][PF_6]$ were added. The mixture was reduced in volume *in vacuo* to precipitate the complex as the hexafluorophosphate salt. Recrystallisation from acetonitrile–water gave [Os(terpy)$_2$][PF_6]$_2$ as a dark powder (0.050 g, 70%). Mass spectrum (FAB, ^{192}Os): *m/z* 803 [Os(terpy)$_2$(PF_6)] and 658 [Os(terpy)$_2$].

[(terpy)Ru(dpqtpy)Ru(dmterpy)][PF_6]$_4$. A suspension of [Ru(terpy)(dpqtpy)][PF_6]$_2$ (0.040 g, 0.037 mmol) and [Ru(dmterpy)Cl_3] (0.018 g, 0.037 mmol) in ethane-1,2-diol (10 cm^3) was heated at reflux for 15 min. The resulting crimson solution was allowed to cool. An equal volume of water was added, along with an excess of methanolic $[NH_4][PF_6]$, to precipitate the complex mixture. This was collected on Celite by filtration, and redissolved in the minimum volume of MeCN and chromatographed over silica [MeCN–saturated aqueous KNO_3–water (7:1:0.5 v/v) as eluent]. The main pink fraction was collected, and water (25 cm^3) and an excess of methanolic $[NH_4][PF_6]$ were added. The mixture was reduced in volume *in vacuo* to precipitate the complex as the hexafluorophosphate salt. Recrystallisation from acetonitrile–water gave [(terpy)Ru(dpqtpy)Ru(dmterpy)][PF_6]$_4$ as a pure red-brown powder (0.023 g, 35%). Mass spectrum (FIB, ^{102}Ru): *m/z* 1613 [(terpy)Ru(dpqtpy)Ru(dmterpy)(PF_6)$_3$], 1467 [(terpy)Ru(dpqtpy)Ru(dmterpy)(PF_6)$_2$], and 1322 [(terpy)Ru(dpqtpy)Ru(dmterpy)(PF_6)].

[(terpy)Ru(dpqtpy)Ru(msterpy)][PF_6]$_4$. The complex [Ru(terpy)(dpqtpy)][PF_6]$_2$ (0.040 g, 0.037 mmol), [Ru(msterpy)Cl_3] (0.019 g, 0.037 mmol) and *N*-ethylmorpholine (three drops) were heated at reflux in methanol (10 cm^3) for 2 h. The resulting red solution was cooled, and then purified by column chromatography over silica [MeCN–saturated aqueous KNO_3–water (7:1:0.5 v/v) as eluent]. The main pink product was collected, and water (25 cm^3) and an excess of methanolic $[NH_4][PF_6]$ were added. The mixture was reduced in volume *in vacuo* to precipitate the complex as the hexafluorophosphate salt. Recrystallisation from acetonitrile–water gave [(terpy)Ru(dpqtpy)Ru(msterpy)][PF_6]$_4$ as a pure red-brown powder (0.022 g, 35%). Mass spectrum (FIB, ^{102}Ru): *m/z* 1647 [(terpy)Ru(dpqtpy)Ru(msterpy)(PF_6)$_3$], 1502 [(terpy)Ru(dpqtpy)Ru(msterpy)(PF_6)$_2$] and 1356 [(terpy)Ru(dpqtpy)Ru(msterpy)(PF_6)].

[(msterpy)Ru(dpqtpy)Ru(dmterpy)][PF_6]$_4$. The complexes [Ru(msterpy)(dpqtpy)][PF_6]$_2$ (0.040 g, 0.034 mmol), [Ru(dmterpy)Cl_3] (0.017 g, 0.034 mmol) and *N*-ethylmorpholine (two drops) were heated at reflux in methanol (10 cm^3) for 1.5 h. The resulting red solution was purified by the same procedure as that for [(terpy)Ru(dpqtpy)Ru(msterpy)][PF_6]$_4$. Recrystallisation from acetonitrile–water gave [(msterpy)Ru(dpqtpy)Ru(dmterpy)][PF_6]$_4$ as a red-brown powder (0.013 g, 21%). Mass spectrum (FAB, ^{102}Ru): *m/z* 1691 [(msterpy)Ru(dpqtpy)Ru(dmterpy)(PF_6)$_3$], 1547 [(msterpy)Ru(dpqtpy)Ru(dmterpy)(PF_6)$_2$]and1401[(msterpy)Ru(dpqtpy)Ru(dmterpy)(PF_6)].

Results and Discussion

We recently described the dinuclear species [(X-terpy)RuLRu(X-terpy)][PF_6]$_4$ (L = dpqtpy or bteb; X-terpy = terpy, pterpy, hterpy, eoterpy, dmterpy, cterpy, mtterpy or msterpy).[8,9] There is a degree of intermetallic interaction; for instance, dinuclear [(terpy)Ru(dpqtpy)Ru(terpy)]$^{4+}$ exhibits λ_{max} 514 nm, 39 nm lower than for the parent [Ru(terpy)$_2$]$^{2+}$ species (λ_{max} 475 nm), although only a single two-electron Ru^{II}–Ru^{III} process is observed at +0.96 V. This is in contrast to the ruthenium centres in [(terpy)Ru(tppz)Ru(terpy)]$^{4+}$ which are oxidised at different potentials.[16] Complexes containing dpqtpy behave similarly, and [(terpy)Ru(dpqtpy)Ru(terpy)]$^{4+}$ shows a single Ru^{II}–Ru^{III} process and λ_{max} 492 nm. The latter absorption spectrum closely resembles that of the related [Ru(pterpy)$_2$]$^{2+}$ complex (λ_{max} 488 nm).[14] Recently, it has been shown that ligands containing conjugated, but spatially distant, terpy domains permit electronic communication over significant distances.[17,18] In an attempt to impose an asymmetry and a redox gradient with ligands such as dpqtpy and bteb, we have adopted a convergent approach to asymmetric homonuclear complexes containing terminator groups ranging from the strongly electron-releasing dmterpy to strongly electron-withdrawing msterpy.

The key requirement was the ligand-*complexes*, [Ru(X-terpy)(dpqtpy)]$^{2+}$, each of which possesses a non-co-ordinated terpy domain. The *terminator complexes*, [Ru(X-terpy)Cl_3], are readily prepared as brown solids by the direct reaction of '$RuCl_3$·*n*H_2O' with X-terpy in methanol, but the reaction of these complexes with dpqtpy in methanol yielded only the dinuclear species [(X-terpy)Ru(dpqtpy)Ru(X-terpy)]$^{4+}$. These were the sole isolable products, irrespective of the ratio of [Ru(X-terpy)Cl_3] to dpqtpy being varied between 0.8 and 2.0:1. However, when the reaction was performed in ethane-1,2-diol with an approximately 1:1 ratio of [Ru(X-terpy)Cl_3] to dpqtpy reasonable yields of mononuclear [Ru(X-terpy)(dpqtpy)]$^{2+}$ complexes were obtained after short periods (Scheme 1).

The use of ethane-1,2-diol as solvent for the reaction has a number of effects on its outcome, not the least being the formation of the desired [Ru(X-terpy)(dpqtpy)]$^{2+}$ complexes. We believe that this is a consequence of the solubilities of the reactants and products in the solvents. Neither dpqtpy nor the complexes [Ru(X-terpy)Cl_3] are particularly soluble in methanol. The initially formed [Ru(X-terpy)(dpqtpy)]$^{2+}$ salts are methanol soluble, and we believe that as a consequence of their higher activity they react with [Ru(X-terpy)Cl_3] in preference to dpqtpy. The result is the formation of only [(X-terpy)Ru(dpqtpy)Ru(X-terpy)]$^{4+}$ in methanol. Both [Ru(X-terpy)

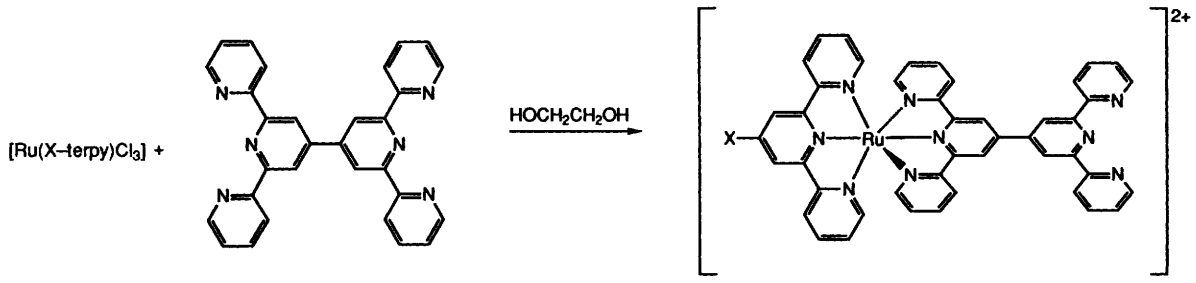

Scheme 1

Cl_3] and dpqtpy are soluble in hot ethane-1,2-diol, although we have no direct information concerning the nature of the purple solution species formed when [Ru(X-terpy)Cl_3] dissolves. The reaction in homogeneous solution gives products which better reflect the stoichiometry of the reactants. We have noted that prolonged reaction times in ethane-1,2-diol result in redistribution reactions giving [(X-terpy)Ru(dpqtpy)Ru(X-terpy)]$^{4+}$ and [Ru(X-terpy)$_2$]$^{2+}$ complexes as the significant products. A second advantage of the use of ethane-1,2-diol is that it reduces the initially formed ruthenium(III) complexes to ruthenium(II), and there is no need to add a reducing agent such as *N*-ethylmorpholine. In ethane-1,2-diol there is little overreduction to ruthenium metal, which is partially responsible for the reduced yields which are sometimes associated with use of *N*-ethylmorpholine.

A ratio of [Ru(X-terpy)Cl_3] to dpqtpy of 0.9:1 and reaction times of 20–30 min were found to optimise the yield of the mononuclear [Ru(X-terpy)(dpqtpy)]$^{2+}$ complexes. Precipitation of a crude mixture of hexafluorophosphate salts followed by column chromatography over silica using a polar mobile phase (MeCN, water, aqueous KNO_3) gave [Ru(X-terpy)(dpqtpy)]$^{2+}$ salts as the first major orange fraction. Dinuclear [(X-terpy)Ru(dpqtpy)Ru(X-terpy)]$^{4+}$ complexes are then collected as a major crimson fraction followed by minor orange and crimson bands identified as [Ru(X-terpy)$_2$]$^{2+}$ and [(X-terpy)Ru(dpqtpy)Ru(dpqtpy)]$^{4+}$ complexes respectively, although neither of the last two species was obtained in significant quantities. This method of preparation and purification proved to be successful for the isolation of the salts [Ru(X-terpy)(dpqtpy)][PF_6]$_2$ (X-terpy = terpy, eoterpy, cterpy or msterpy), but chromatographic methods were not suitable for the purification of [Ru(dmterpy)(dpqtpy)][PF_6]$_2$. Accordingly, we used our previously developed methodology involving a metal-directed reaction of a co-ordinated 4-chloropyridine for the *in situ* generation of the dmterpy ligand.[14,19] The reaction of [Ru(cterpy)(dpqtpy)][PF_6]$_2$ with a solution of dimethylamine in methanol (33% w/w) at ambient temperature resulted in the formation of mixtures of [Ru(dmterpy)(dpqtpy)]$^{2+}$ and [Ru(moterpy)(dpqtpy)]$^{2+}$ salts, and it was necessary to use anhydrous dimethylamine at 0 °C to achieve a clean conversion into [Ru(dmterpy)(dpqtpy)]$^{2+}$ (Scheme 2).

The ligand-complexes [Ru(X-terpy)(dpqtpy)][PF_6]$_2$ (X-terpy = terpy, eoterpy, cterpy, msterpy or dmterpy) have been characterised by partial elemental analysis (Table 1), mass spectrometry and ^{1}H NMR spectroscopy, and their electrochemical and electronic spectroscopic properties investigated. In each case, the FAB mass spectrum (Table 2) contains isotopomeric clusters of peaks corresponding to {[(X-terpy)Ru(dpqtpy)][PF_6]}$^+$ and {[(X-terpy)Ru(dpqtpy)]}$^+$. In some cases, a peak at *m/z* 565 assigned to {Ru(dpqtpy)}$^+$ is also observed. The ^{1}H NMR spectra of CD_3CN solutions of each complex exhibit resonances which may be assigned to three different terpy groups (Fig. 1); one set results from the X-terpy ligand, and one set due to each of the co-ordinated and non-co-ordinated domains of the dpqtpy (Table 3). Assignments have been made from correlation spectroscopy (COSY) experiments, and by comparison with the spectra of symmetric [(Ru(X-terpy)$_2$]$^{2+}$ and [(X-terpy)Ru(dpqtpy)Ru(X-terpy)]$^{4+}$ complexes. We have previously reported the NMR data for these complexes in CD_3COCD_3 solution[8,9,14] and now include in Table 3 chemical shift data in CD_3CN solution, to allow direct comparison. We have discussed in earlier papers the co-ordination shifts of these ligands upon co-ordination to ruthenium(II) and also the conservancy of chemical shift values for a given ligand in an {Ru(terpy)$_2$} environment, and these trends are generally applicable to these new complexes.[8,9,14] A number of trends are apparent for the X-terpy terminator ligands. The increase in charge upon going from [Ru(X-terpy)$_2$]$^{2+}$ to [(X-terpy)Ru(dpqtpy)Ru(X-terpy)]$^{4+}$ results in a small downfield shift; the average shift is δ +0.07 with the greatest variation being observed for H^6. The effect of the charge may be probed by considering the resonances of the X-terpy groups in the complexes [Ru(X-terpy)(dpqtpy)]$^{2+}$; once again there is a small downfield shift upon going from [Ru(X-terpy)$_2$]$^{2+}$ to [Ru(X-terpy)(dpqtpy)]$^{2+}$. Table 2 reveals that the effect of increasing the charge from 2+ to 4+ is actually minimal, with at least half of the difference in chemical shift between [Ru(X-terpy)$_2$]$^{2+}$ to [(X-terpy)Ru(dpqtpy)Ru(X-terpy)]$^{4+}$ resulting from the introduction of the dpqtpy ligand. In general, the chemical shifts of the X-terpy ligands in [Ru(X-terpy)(dpqtpy)]$^{2+}$ lie half-way between those in [Ru(X-terpy)$_2$]$^{2+}$ and [(X-terpy)Ru(dpqtpy)Ru(X-terpy)]$^{4+}$. The same charge effects are observed in the co-ordinated domains of the dpqtpy ligands. The resonances assigned to the dpqtpy ligand in [(X-terpy)Ru(dpqtpy)Ru(X-terpy)]$^{4+}$ lie downfield of those assigned to the co-ordinated domain of the dpqtpy in [Ru(X-terpy)(dpqtpy)]$^{2+}$. Perhaps most significantly, the resonances assigned to the non-co-ordinated terpy domains in [Ru(X-terpy)(dpqtpy)]$^{2+}$ exhibit similar chemical shifts to those of free terpy in acetonitrile solution, but with a downfield shift of δ 0.1–0.25 attributed to the charge on the complex.

Acetonitrile solutions of the [Ru(X-terpy)(dpqtpy)]$^{2+}$ complexes are electrochemically active and exhibit a Ru^{II}–Ru^{III} process, and two quasi-reversible ligand-centred reductions (Table 4). The Ru^{II}–Ru^{III} oxidation potentials vary from 0.60 V for the strongly electron-releasing dmterpy ligand to 1.06 V for electron-withdrawing msterpy. These potentials are essentially identical to those for the corresponding dinuclear complexes [(X-terpy)Ru(dpqtpy)Ru(X-terpy)]$^{4+}$.[8,9] This is further evidence that the oxidation potential of the ruthenium centres in [(X-terpy)Ru(dpqtpy)Ru(X-terpy)]$^{4+}$ is solely a function of the nature of the two ligands (X-terpy and dpqtpy) and that there are minimal intermetallic effects. The complexes exhibit intense (ε 24 000 dm^3 mol^{-1} cm^{-1}) metal-to-ligand charge-transfer (m.l.c.t.) transitions in their electronic spectra, with λ_{max} in the range 482–499 nm (Table 5). These λ_{max} values are 8–38 nm higher in energy than for the corresponding [(X-terpy)Ru(dpqtpy)Ru(X-terpy)]$^{4+}$ complexes, which suggests that, in the dinuclear complexes, the two metal centres interact to stabilise the lowest excited m.l.c.t. level. This explains the subjective observations that acetonitrile solutions of [Ru(X-terpy)(dpqtpy)]$^{2+}$ complexes are orange whilst those of [(X-terpy)Ru(dpqtpy)Ru(X-terpy)]$^{4+}$ salts are pink. The λ_{max} values of the [Ru(X-terpy)(dpqtpy)]$^{2+}$ complexes are in fact identical to those for the corresponding [Ru(X-terpy)(pterpy)]$^{2+}$ species.[14] This is to be expected as dpqtpy co-

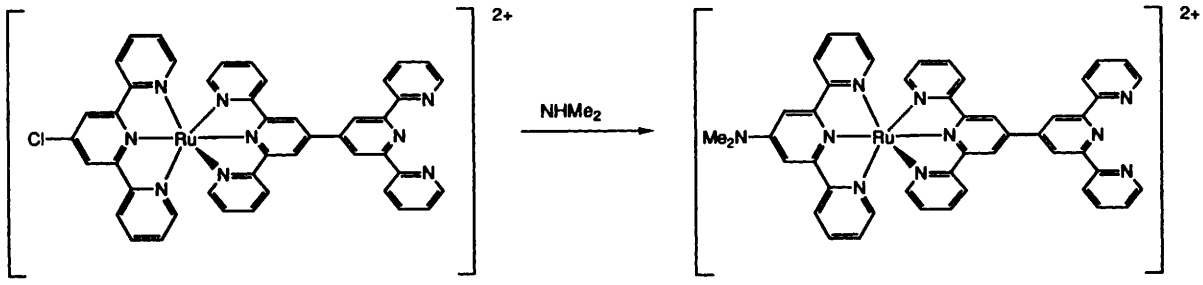

Scheme 2

Table 1 Partial elemental analysis data for complexes

		Analysis (%)					
		Found			Calc.		
Complex	M_r	C	H	N	C	H	N
$[Ru(terpy)(dpqtpy)][PF_6]_2$	1088.8	48.50	3.15	11.05	49.65	2.85	11.60
$[Ru(eoterpy)(dpqtpy)][PF_6]_2$	1132.9	48.30	3.00	10.75	49.80	3.10	11.15
$[Ru(dmterpy)(dpqtpy)][PF_6]_2$	1131.9	48.65	3.00	12.00	49.85	3.20	12.40
$[Ru(cterpy)(dpqtpy)][PF_6]_2$	1123.3	47.15	2.85	11.05	48.10	2.65	11.20
$[Ru(msterpy)(dpqtpy)][PF_6]_2$	1166.9	45.90	3.00	10.20	47.35	2.85	10.80
$[(terpy)Ru(dpqtpy)Fe(dpqtpy)Ru(terpy)][PF_6]_6$	2522.4	42.00	2.75	9.25	42.80	2.45	10.00
$[(eoterpy)Ru(dpqtpy)Fe(dpqtpy)Ru(eoterpy)][PF_6]_6$	2611.5	42.50	3.20	8.55	43.20	2.70	9.65
$[(dmterpy)Ru(dpqtpy)Fe(dpqtpy)Ru(dmterpy)][PF_6]_6$	2609.5	43.10	2.90	10.40	43.25	2.75	10.75
$[(cterpy)Ru(dpqtpy)Fe(dpqtpy)Ru(cterpy)][PF_6]_6$	2592.3	41.15	3.00	8.55	41.70	2.30	9.75
$[(msterpy)Ru(dpqtpy)Fe(dpqtpy)Ru(msterpy)][PF_6]_6$	2679.5	41.00	2.90	8.65	41.20	2.45	9.40
$[(terpy)Ru(dpqtpy)Co(dpqtpy)Ru(terpy)][PF_6]_6$	2526.5	42.35	2.70	9.70	42.75	2.45	10.00
$[(terpy)Ru(dpqtpy)Co(dpqtpy)Ru(terpy)][PF_6]_7$	2671.4	40.35	2.45	9.15	40.45	2.30	9.45
$[(terpy)Ru(dpqtpy)Ru(dpqtpy)Ru(terpy)][PF_6]_6$	2568.6	40.30	2.75	8.75	42.05	2.40	9.80
$[(terpy)Ru(dpqtpy)Os(terpy)][PF_6]_4$	1802.2	39.75	2.60	9.25	40.00	2.35	9.35
$[(terpy)Os(dpqtpy)Os(terpy)][PF_6]_4$	1891.3	37.15	2.45	8.10	38.10	2.20	8.90
$[Os(terpy)_2][PF_6]_2$	946.7	38.25	2.25	8.90	38.05	2.35	8.90
$[(terpy)Ru(dpqtpy)Ru(dmterpy)][PF_6]_4$	1756.1	40.40	2.45	9.75	42.40	2.70	10.35
$[(terpy)Ru(dpqtpy)Ru(msterpy)][PF_6]_4$	1791.2	40.10	2.50	9.25	40.90	2.45	9.40
$[(msterpy)Ru(dpqtpy)Ru(dmterpy)][PF_6]_4$	1834.2	39.25	2.70	9.20	41.25	2.65	9.95

Table 2 Mass spectrometric data for $[Ru(X\text{-}terpy)(dpqtpy)][PF_6]_2$ and $[(X\text{-}terpy)Ru(dpqtpy)Fe(dpqtpy)Ru(X\text{-}terpy)][PF_6]_6$ complexes, for major isotopomer (calculated values in parentheses)

		m/z		
Complex		$M^+ - PF_6$	$M^+ - 2PF_6$	Others
$[Ru(terpy)(dpqtpy)][PF_6]_2$	FAB	944 (944)	799 (799)	—
$[Ru(eoterpy)(dpqtpy)][PF_6]_2$	FAB	989 (988)	844 (843)	$[Ru(dpqtpy)]^+$ 565 (566)
$[Ru(dmterpy)(dpqtpy)][PF_6]_2$	FAB	988 (987)	842 (842)	$[Ru(dpqtpy)]^+$ 566 (566)
$[Ru(cterpy)(dpqtpy)][PF_6]_2$	FAB	979 (978)	833 (833)	$[Ru(dpqtpy)]^+$ 564 (566)
$[Ru(msterpy)(dpqtpy)][PF_6]_2$	FAB	1023 (1022)	877 (877)	$[Ru(dpqtpy)]^+$ 564 (566)
		$\{[(X\text{-}terpy)Ru(dpqtpy)][PF_6]\}^+$		$[(X\text{-}terpy)Ru(dpqtpy)]^+$
$[(terpy)Ru(dpqtpy)Fe(dpqtpy)Ru(terpy)][PF_6]_6$	FIB	943 (944)		798 (799)
$[(eoterpy)Ru(dpqtpy)Fe(dpqtpy)Ru(eoterpy)][PF_6]_6$	FIB	987 (988)		842 (843)*
$[(dmterpy)Ru(dpqtpy)Fe(dpqtpy)Ru(dmterpy)][PF_6]_6$	FIB	986 (987)		841 (842)
$[(cterpy)Ru(dpqtpy)Fe(dpqtpy)Ru(cterpy)][PF_6]_6$	FIB	—		833 (833)
$[(msterpy)Ru(dpqtpy)Fe(dpqtpy)Ru(msterpy)][PF_6]_6$	FIB	1022 (1022)		877 (877)

* [(oeterpy)Ru(dpqtpy)] *m/z* 814 (814)

ordinated in a mononuclear fashion is effectively a terpy bearing a conjugated substituent group in the 4′ position. The absorption coefficients for the $[Ru(X\text{-}terpy)(dpqtpy)]^{2+}$ species are typically 3000 $dm^3\ mol^{-1}\ cm^{-1}$ greater than those for $[Ru(X\text{-}terpy)(pterpy)]^{2+}$, as expected given the higher degree of conjugation in dpqtpy.

Having prepared the *ligand-complexes* $[Ru(X\text{-}terpy)(dpqtpy)]^{2+}$ we then investigated the ability of the non-co-ordinated terpy domain to bind to a second metal centre (Scheme 3). Acetonitrile solutions of $[Ru(X\text{-}terpy)(dpqtpy)]^{2+}$ (X-terpy = terpy, eoterpy, msterpy, cterpy or dmterpy) react instantly with aqueous $[Fe(H_2O)_6][BF_4]_2$ to form $[(X\text{-}terpy)Ru(dpqtpy)Fe(dpqtpy)Ru(X\text{-}terpy)]^{6+}$ complexes. This is associated with a colour change from orange to purple as a result of the formation of the $\{Fe(terpy)_2\}$ chromophore in the complex. The complexes were isolated as the dark red-brown diamagnetic salts $[(X\text{-}terpy)Ru(dpqtpy)Fe(dpqtpy)Ru(X\text{-}terpy)][PF_6]_6$. The ^1H NMR spectra of CD_3CN solutions show three sets of resonances (Table 3) assigned to three different terpy domains (Fig. 2): specifically to the X-terpy, and the two different terpy domains of dpqtpy, one of which is co-ordinated to a ruthenium centre and the other to the iron centre. It is relevant that the observation of three rather than six sets of terpy resonances confirms that, in solution, the molecule is symmetrical about the iron centre. The resonances are not paramagnetically shifted or broadened, so the iron also

Table 3 Proton NMR data for the complexes. All coupling constants are typical for 2,2′:6′,2″-terpyridines [$J(H^5H^6) \approx 6$; $J(H^3H^4) \approx J(H^4H^5) \approx 7$ Hz]

	(X-terpy)Ru					
Compound	H^3	H^4	H^5	H^6	$H^{3'}$	Others
$[Ru(terpy)_2][PF_6]_2$	8.48	7.91	7.15	7.33	8.74	8.40 ($H^{4'}$)
$[Ru(eoterpy)_2][PF_6]_2$	8.46	7.88	7.13	7.37	8.27	4.58 (CH_2), 1.64 (Me)
$[Ru(dmterpy)_2][PF_6]_2$	8.45	7.83	7.11	7.37	7.91	3.44 (Me)
$[Ru(cterpy)_2][PF_6]_2$	8.47	7.94	7.19	7.49	8.84	
$[Ru(msterpy)_2][PF_6]_2$	8.68	7.98	7.23	7.40	9.15	3.52 (Me)
[(terpy)Ru(dpqtpy)Ru(terpy)][PF_6]$_4$	8.57	8.00	7.21	7.47	8.82	8.50 ($H^{4'}$)
[(eoterpy)Ru(dpqtpy)Ru(eoterpy)][PF_6]$_4$	8.54	7.95	7.19	7.44	8.36	4.65 (CH_2), 1.68 (Me)
[(dmterpy)Ru(dpqtpy)Ru(dmterpy)][PF_6]$_4$	8.54	7.91	7.12	7.35	7.99	3.51 (Me)
[(cterpy)Ru(dpqtpy)Ru(cterpy)][PF_6]$_4$	8.55	8.00	7.26	7.50	8.92	
[(msterpy)Ru(dpqtpy)Ru(msterpy)][PF_6]$_4$	8.74	8.04	7.32	7.58	9.20	3.55 (Me)
terpy						
$[Ru(terpy)(dpqtpy)][PF_6]_2$	8.51	7.93	7.18	7.45	8.78	8.44 ($H^{4'}$)
$[Ru(eoterpy)(dpqtpy)][PF_6]_2$	8.49	7.91	7.14	7.47	8.32	4.62 (CH_2), 1.66 (Me)
$[Ru(dmterpy)(dpqtpy)][PF_6]_2$	8.49	7.86	7.08	7.32	7.95	3.48 (Me)
$[Ru(cterpy)(dpqtpy)][PF_6]_2$	8.50	7.96	7.20	7.48	8.87	
$[Ru(msterpy)(dpqtpy)][PF_6]_2$	8.69	7.99	7.27	7.54	9.15	3.52 (Me)
[(terpy)Ru(dpqtpy)Fe(dpqtpy)Ru(terpy)][PF_6]$_6$	8.57	8.00	7.26	7.53	8.83	8.50 ($H^{4'}$)
[(eoterpy)Ru(dpqtpy)Fe(dpqtpy)Ru(eoterpy)][PF_6]$_6$	8.56	7.98	7.24	7.48	8.38	4.66 (CH_2), 1.69 (Me)
[(dmterpy)Ru(dpqtpy)Fe(dpqtpy)Ru(dmterpy)][PF_6]$_6$	8.56	7.94	7.16	7.39	8.01	3.52 (Me)
[(cterpy)Ru(dpqtpy)Fe(dpqtpy)Ru(cterpy)][PF_6]$_6$	8.56	8.02	7.29	7.55	8.93	
[(msterpy)Ru(dpqtpy)Fe(dpqtpy)Ru(msterpy)][PF_6]$_6$	8.76	8.09	7.36	7.62	9.22	3.56 (Me)
[(terpy)Ru(dpqtpy)Co(dpqtpy)Ru(terpy)][PF_6]$_7$	8.57	7.99	7.25	7.50	8.83	8.51 ($H^{4'}$)
[(terpy)Ru(dpqtpy)Ru(dpqtpy)Ru(terpy)][PF_6]$_6$	8.56	7.99	7.25	7.51	8.83	8.50 ($H^{4'}$)
[(terpy)Ru(dpqtpy)Os(terpy)][PF_6]$_4$	8.56	7.98	7.25	7.49	8.83	8.48 ($H^{4'}$)
[(terpy)Os(dpqtpy)Os(terpy)][PF_6]$_4$						
$[Os(terpy)_2][PF_6]_2$						
[(terpy)Ru(dpqtpy)Ru(dmterpy)][PF_6]$_4$	8.55	7.98	7.23	7.48	8.81	8.48 ($H^{4'}$)
[(terpy)Ru(dpqtpy)Ru(msterpy)][PF_6]$_4$	8.56	7.98	7.23	7.48	8.82	8.49 ($H^{4'}$)
[(msterpy)Ru(dpqtpy)Ru(dmterpy)][PF_6]$_4$	8.74	8.04	7.33	7.58	9.20	3.55 (Me)

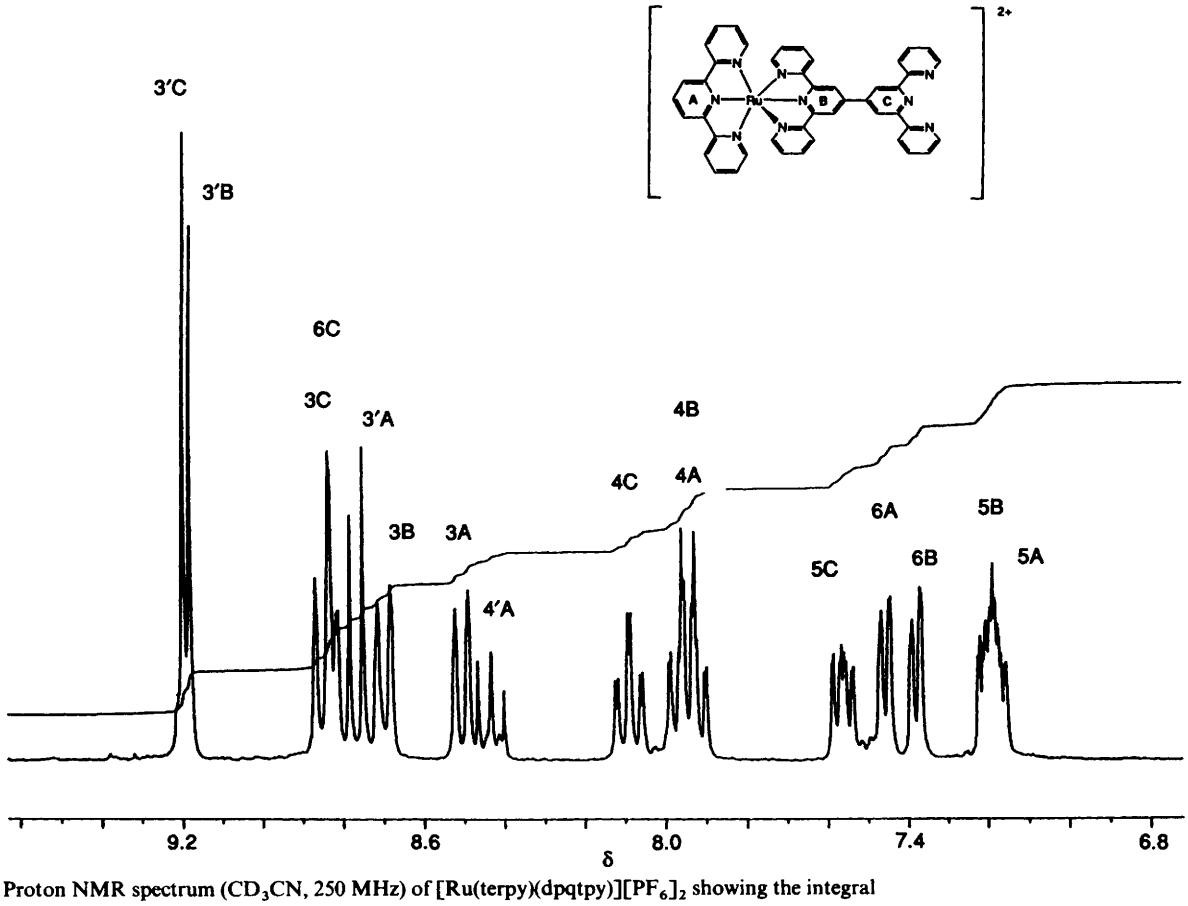

Fig. 1 Proton NMR spectrum (CD_3CN, 250 MHz) of $[Ru(terpy)(dpqtpy)][PF_6]_2$ showing the integral

Table 3 (*Continued*)

Ru(dpqtpy)					Ru(dpqtpy)M					Unco-ordinated terpy					
H^3	H^4	H^5	H^6	$H^{3'}$	H^3	H^4	H^5	H^6	$H^{3'}$	H^3	H^4	H^5	H^6	$H^{3'}$	Others
8.90	8.10	7.29	7.48	9.48											
8.86	8.07	7.30	7.55	9.44											
8.86	8.07	7.34	7.61	9.42											
8.85	8.08	7.28	7.50	9.44											
8.87	8.07	7.26	7.45	9.49											
										8.66	7.95	7.42	8.69	8.54	8.02 ($H^{4'}$)
8.73	7.97	7.20	7.38	9.23						8.89	8.14	7.61	8.83	9.23	
8.69	7.95	7.23	7.41	9.18						8.85	8.08	7.55	8.82	9.18	
8.69	7.95	7.25	7.53	9.14						8.83	8.08	7.55	8.81	9.19	
8.69	7.96	7.20	7.41	9.18						8.85	8.08	7.55	8.82	9.18	
8.69	7.96	7.17	7.36	9.20						8.85	8.08	7.55	8.82	9.20	
8.91	8.09	7.30	7.50	9.68	8.87	8.09	7.26	7.39	9.58						
8.89	8.09	7.34	7.59	9.67	8.86	8.09	7.24	7.38	9.56						
8.89	8.09	7.29	7.65	9.67	8.86	8.09	7.26	7.39	9.54						
8.89	8.09	7.29	7.55	9.67	8.86	8.09	7.29	7.38	9.57						
8.90	8.09	7.28	7.49	9.68	8.86	8.09	7.28	7.38	9.60						
8.85	8.10	7.31	7.50	9.72	8.93	8.43	7.65	7.62	9.51						
8.89	8.08	7.28	7.48	9.50	8.93	8.13	7.36	7.63	9.53						
										M(X-terpy)					
8.88	8.07	7.28	7.45	9.43	8.84	7.94	7.22	7.37	9.43	8.52	7.83	7.15	7.33	8.81	8.03 ($H^{4'}$)
					8.86	7.93	7.21	7.35	9.43	8.53	7.83	7.16	7.35	8.83	8.02 ($H^{4'}$)
										8.45	7.76	7.07	7.20	8.74	7.92 ($H^{4'}$)
8.85	8.07	7.27	7.46	9.44	8.85	8.07	7.34	7.61	9.41	8.55	7.92	7.13	7.35	7.99	3.51 (Me)
8.88	8.08	7.28	7.48	9.47	8.88	8.08	7.26	7.48	9.49	8.75	8.04	7.33	7.59	9.20	3.55 (Me)
8.85	8.07	7.26	7.46	9.46	8.85	8.07	7.35	7.62	9.41	8.55	7.92	7.13	7.35	7.99	3.51 (Me)

Table 4 Electrochemical data (V) for the complexes (MeCN solvent, $[NBu^n_4][BF_4]$ supporting electrolyte, *versus* internal ferrocene–ferrocenium)

	Oxidations		Reductions
Complex	Ru^{II}–Ru^{III}	Others	
$[Ru(terpy)(dpqtpy)][PF_6]_2$	0.98		−1.56, −1.89
$[Ru(eoterpy)(dpqtpy)][PF_6]_2$	0.86		−1.56, −1.88
$[Ru(dmterpy)(dpqtpy)][PF_6]_2$	0.60		−1.62, −2.02
$[Ru(cterpy)(dpqtpy)][PF_6]_2$	0.98		−1.53, −1.77
$[Ru(msterpy)(dpqtpy)][PF_6]_2$	1.06		−1.40, −1.75
		Fe^{II}–Fe^{III}	
$[(terpy)Ru(dpqtpy)Fe(dpqtpy)Ru(terpy)][PF_6]_6$	0.97	0.80	−1.27, −1.35, −1.68, −1.81
$[(eoterpy)Ru(dpqtpy)Fe(dpqtpy)Ru(eoterpy)][PF_6]_6$	0.86[a]	0.86[a]	−1.25, −1.34, −1.65, −1.83
$[(dmterpy)Ru(dpqtpy)Fe(dpqtpy)Ru(dmterpy)][PF_6]_6$	0.61	0.84	−1.32, −1.40, −1.73, −2.00
$[(cterpy)Ru(dpqtpy)Fe(dpqtpy)Ru(cterpy)][PF_6]_6$	1.03	0.82	−1.27, −1.35, −1.66, −1.78
$[(msterpy)Ru(dpqtpy)Fe(dpqtpy)Ru(msterpy)][PF_6]_6$	1.04	0.79	−1.31, −1.45, −1.75
$[(terpy)Ru(dpqtpy)Co^{II}(dpqtpy)Ru(terpy)][PF_6]_6$	0.96		−1.40, −1.55, −1.85
$[(terpy)Ru(dpqtpy)Co^{III}(dpqtpy)Ru(terpy)][PF_6]_7$	0.94		*b*
$[(terpy)Ru(dpqtpy)Ru(dpqtpy)Ru(terpy)][PF_6]_6$	0.98[c]		−1.29, −1.39[d]
		Os^{II}–Os^{III}	
$[(terpy)Ru(dpqtpy)Os(terpy)][PF_6]_4$	0.95	0.59	−1.36, −1.65[d]
$[(terpy)Os(dpqtpy)Os(terpy)][PF_6]_4$		0.62	−1.38, −1.63, −1.86
$[Os(terpy)_2][PF_6]_2$		0.58	−1.63, −1.95
$[(terpy)Ru(dpqtpy)Ru(dmterpy)][PF_6]_4$	0.60,[e] 0.96[f]		−1.39, −1.71[d]
$[(terpy)Ru(dpqtpy)Ru(msterpy)][PF_6]_4$	0.97,[f] 1.07[g]		−1.29, −1.48[d]
$[(dmterpy)Ru(dpqtpy)Ru(msterpy)][PF_6]_4$	0.60,[e] 1.05[g]		−1.34, −1.51, −1.82, −2.08

[a] The Fe^{II}–Fe^{III} and Ru^{II}–Ru^{III} processes are at very similar potentials and could not be resolved. [b] Reductive processes are poorly resolved. [c] All the Ru^{II}–Ru^{III} processes at similar potentials. [d] Further processes obscured by an absorption spike. [e] Ru(dmterpy). [f] Ru(terpy). [g] Ru(msterpy).

possesses the low-spin d^6 electronic configuration in solution. Mass spectrometry has not been of significant use in the characterisation of these complexes, as FAB, FIB and laser-desorption time-of-flight spectra all display $\{[X\text{-terpy})\text{-}Ru(dpqtpy)][PF_6]\}^+$ as the highest-mass peak. This is presumably due to easy fragmentation at the comparatively labile central iron(II) centre (Table 2). Partial elemental analysis (Table 1) does, however, provide confirmation of the proposed stoichiometry.

All five $[(X\text{-terpy})Ru(dpqtpy)Fe(dpqtpy)Ru(X\text{-terpy})]^{6+}$

Table 5 Electronic spectroscopic data for the complexes (MeCN solution), λ_{max}/nm (10^{-3} ε/dm^3 mol^{-1} cm^{-1})

Complex		X-terpy				
		terpy	eoterpy	dmterpy	cterpy	msterpy
[Ru(X-terpy)(dpqtpy)][PF$_6$]$_2$		482 (23.1)	489 (23.4)	499 (23.9)	484 (24.4)	487.5 (26.4)
[(X-terpy)Ru(dpqtpy)Fe(dpqtpy)Ru(X-terpy)][PF$_6$]$_6$	Ru m.l.c.t.	489 (42.6)	496 (43.6)	507 (38.1)	489 (44.0)	491 (55.6)
	Fe m.l.c.t.	595 (65.0)	596 (66.4)	598 (64.0)	597 (59.4)	595.5 (69.1)
[(terpy)Ru(dpqtpy)M(dpqtpy)Ru(terpy)][PF$_6$]$_n$	Ru m.l.c.t.	497.4 (49.1)(M = Co^{II}) 514(41.5)(M = Co^{III}) 525(82.8)(M = Ru^{II})				
[(terpy)Ru(dpqtpy)Ru(dmterpy)][PF$_6$]$_4$		527(52.9), 526(56.0)				
[(terpy)Ru(dpqtpy)Ru(msterpy)][PF$_6$]$_4$		510(56.7), 511(54.8)				
[(msterpy)Ru(dpqtpy)Ru(dmterpy)][PF$_6$]$_4$		527(56.9), 523(61.1)				
[(terpy)Ru(dpqtpy)Os(terpy)][PF$_6$]$_4$		515(41.0), 671(5.8)				
[(terpy)Os(dpqtpy)Os(terpy)][PF$_6$]$_4$		519(43.8), 685(16.2)				
[Os(terpy)$_2$][PF$_6$]$_2$		475(15.4), 656(4.2)				

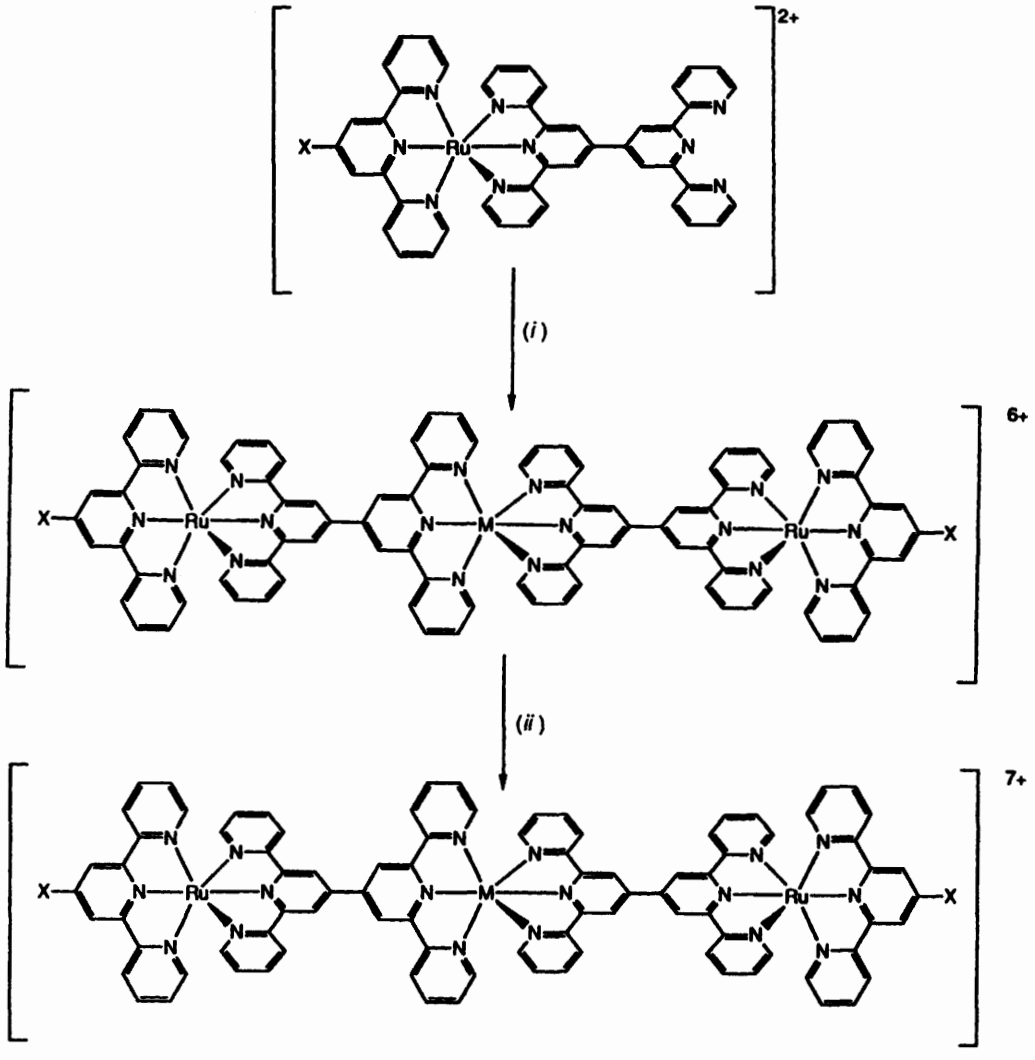

Scheme 3 (*i*) $RuCl_3$, M = Ru; Fe^{2+}, M = Fe; Co^{2+}, M = Co; (*ii*) M = Co, Cl_2

complexes are electrochemically active (Table 4), and exhibit two quasi-reversible metal-centred processes. The first of these is a one-electron process corresponding to the Fe^{II}–Fe^{III} couple, and the second is a two-electron process involving the Ru^{II}–Ru^{III} couple (Fig. 3). As expected from the behaviour of [(X-terpy)Ru(dpqtpy)Ru(X-terpy)]$^{4+}$, only a single Ru^{II}–Ru^{III} process is observed. A variety of ligand-centred reductive processes is also observed. The potential of the Ru^{II}–Ru^{III} couple is controlled by the X-terpy ligand, and varies in the range 0.61–1.04 V upon moving from the electron-releasing dmterpy ligand to electron-withdrawing msterpy. Once again, in each case this couple is at a similar potential to that observed in the appropriate [(X-terpy)Ru(dpqtpy)Ru(X-terpy)]$^{4+}$ complex. Significantly, the Fe^{II}–Fe^{III} process at 0.83 ± 0.03 V is not

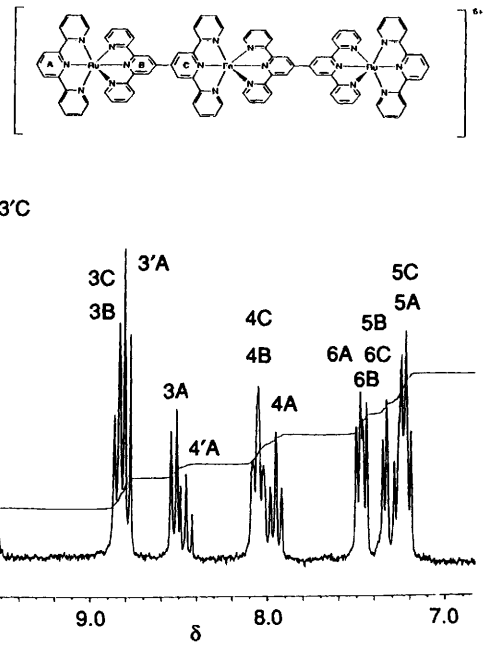

Fig. 2 Proton NMR spectrum (CD_3CN, 250 MHz) of [(terpy)-Ru(dpqtpy)Fe(dpqtpy)Ru(terpy)][PF_6]$_6$

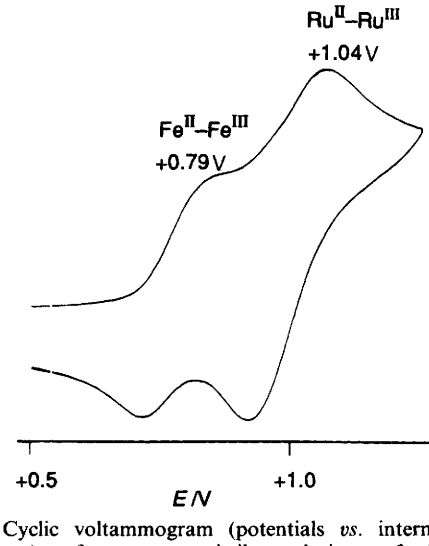

Fig. 3 Cyclic voltammogram (potentials *vs.* internal ferrocene–ferrocenium) of an acetonitrile solution of [(msterpy)Ru-(dpqtpy)Fe(dpqtpy)Ru(msterpy)][PF_6]$_6$

affected by the variation of the X-terpy ligand on the remote ruthenium centres.

These five heterotrinuclear complexes exhibit interesting electronic spectra. Two low-energy m.l.c.t. bands are observed (Table 5), one associated with the iron(II) centre and the other with the ruthenium(II) centres. As noted above in our discussion of the electrochemical behaviour, the iron centre is not sensitive to the X-terpy ligands, and the iron(II) m.l.c.t. bands are not significantly shifted upon variation of the X-terpy ligand (λ_{max} 596.5 ± 1.5 nm for the five complexes investigated). This compares with λ_{max} 569 nm (ε 24 500 dm^3 mol^{-1} cm^{-1}) for [Fe(pyterpy)$_2$]$^{2+}$ and with λ_{max} 595 nm (ε 25 700 dm^3 mol^{-1} cm^{-1}) for [Fe(mpyterpy)$_2$]$^{4+}$.[7] In [Fe(pyterpy)$_2$]$^{2+}$, pyterpy is a potentially dinucleating ligand which co-ordinates to iron(II) through a terpy domain leaving a non-co-ordinated pyridine ring on each ligand which can be methylated or protonated. The shift of λ_{max} to lower energy upon methylation is comparable to the effect of metallation, and it is notable that the absorption maximum of [Fe(mpyterpy)$_2$]$^{4+}$ closely resembles that of the heterotrinuclear complexes. It is of interest that the absorption coefficients for the iron(II) m.l.c.t. bands (ε 59 400–69 100 dm^3 mol^{-1} cm^{-1}) are approximately 2.5 times those for mononuclear complexes. The ruthenium-centred m.l.c.t. transitions vary in the range λ_{max} 489–507 nm, and are at approximately 20 nm shorter wavelength than for the analogous dinuclear complexes [(X-terpy)Ru(dpqtpy)Ru(X-terpy)]$^{4+}$. The absorption coefficients for the ruthenium(II) transition are slightly lower than those for the dinuclear analogues. For example, in [(terpy)-Ru(dpqtpy)Fe(dpqtpy)Ru(terpy)]$^{6+}$ the two ruthenium-centred m.l.c.t. transitions are found at λ_{max} 489 nm (ε 42 600 dm^3 mol^{-1} cm^{-1}) whilst for the dinuclear analogue [(terpy)-Ru(dpqtpy)Ru(terpy)]$^{4+}$ they are found at λ_{max} 514 nm (ε 49 600 dm^3 mol^{-1} cm^{-1}). We have discussed a possible origin for these effects in detail elsewhere.[10,20]

The analogous heterotrinuclear diruthenium(II)cobalt(II) complexes [(terpy)Ru(dpqtpy)Co^{II}(dpqtpy)Ru(terpy)]$^{6+}$ can also be prepared by mixing aqueous cobalt(II) acetate with an acetonitrile solution of the *ligand-complex* [Ru(terpy)-(dpqtpy)]$^{2+}$. An immediate colour change from orange to pink results. Following the addition of an excess of methanolic [NH_4][PF_6] the brown hexafluorophosphate salt [(terpy)-Ru(dpqtpy)Co^{II}(dpqtpy)Ru(terpy)][PF_6]$_6$ is obtained in 84% yield. The corresponding cobalt(III) species, [(terpy)Ru-(dpqtpy)Co^{III}(dpqtpy)Ru(terpy)]$^{7+}$, is prepared by oxidation of a crude solution of the cobalt(II) complex solution with chlorine, and may be isolated as the pink-brown hexafluorophoshate salt [(terpy)Ru(dpqtpy)Co^{III}(dpqtpy)Ru(terpy)]-[PF_6]$_7$. In these reactions we have utilised the labile d^7 cobalt(II) centre to allow the rapid and near-quantitative formation of the heterotrinuclear complex, and then generated the kinetically inert d^6 cobalt(III) complex *in situ*.

Although the complexes gave satisfactory partial elemental analyses, mass spectrometry was not of significant use in their further characterisation. In general they exhibit fragmentation peaks, with {[(terpy)Ru(dpqtpy)][PF_6]}$^+$ as the highest-mass observed peak, even in the case of the complex containing kinetically inert cobalt(III). The ^{1}H NMR spectra of the complexes are, however, characteristic and informative. The d^7 configuration of cobalt(II) results in paramagnetic shifting and broadening of the peaks in the ^{1}H NMR spectrum of [(terpy)Ru(dpqtpy)Co^{II}(dpqtpy)Ru(terpy)][PF_6]$_6$ (Fig. 4). We have previously made extensive use of the shifted ^{1}H NMR spectra of cobalt(II) complexes of related ligands to characterise the solution behaviour of the complexes.[21] As expected, 16 resonances are observed in the ^{1}H NMR spectrum of [(terpy)Ru(dpqtpy)Co^{II}(dpqtpy)Ru(tpy)][PF_6]$_6$. Five of these, at δ 95, 55, 42, 34 and 14.4, are significantly paramagnetically shifted and are assigned to the five proton resonances of the terpy domain which is co-ordinated to the cobalt(II) centre. These are observed as broad resonances with no observable coupling. Although we have not been able unambiguously to assign these resonances, they correspond very closely to the shifted resonances observed in the ^{1}H NMR spectrum of the model complex [Co^{II}(pterpy)$_2$]$^{2+}$.[22] The remaining 11 resonances are only slightly shifted and may be assigned to the two terpy domains co-ordinated to the ruthenium(II) centres. These resonances are observed at δ 10.1 (d, H^{3}), 9.45 (br s, H$^{3'}$, dpqtpy), 9.01 (d, H$^{3'}$, terpy), 8.90 (d, H^{3}), 8.63 (t, H$^{4'}$, terpy), 8.61 (d, H^{6}), 8.58 (dd, H^{4}), 8.21 (dd, H^{4}), 7.95 (d, H^{6}), 7.71 (dd, H^{5}) and 7.56 (dd, H^{5}). Six of these resonances are due to the terminal terpy ligand, and five to the terpy domain of dpqtpy that is co-ordinated to the ruthenium(II) centres. Paramagnetic broadening is slight, and the primary couplings within these spin systems are resolved. We have not been able, however, unambiguously to assign the two four-proton spin systems to the terpy domains of the dpqtpy or the terpy ligand.

In contrast, the complex [(terpy)Ru(dpqtpy)Co^{III}(dpqtpy)-Ru(terpy)][PF_6]$_7$ is diamagnetic, and exhibits 16 resonances in its ^{1}H NMR spectrum. These possess 'normal' chemical shifts

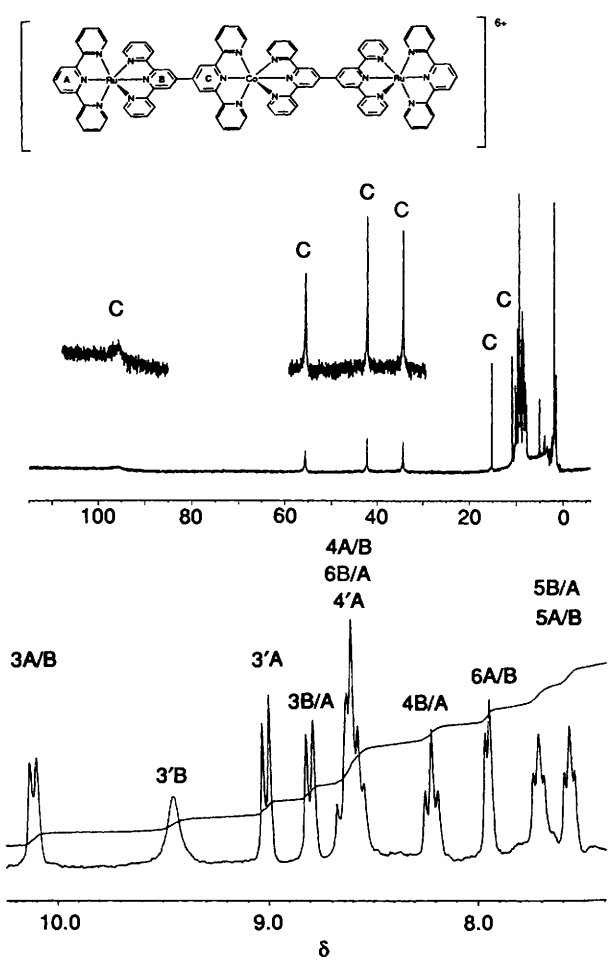

Fig. 4 Proton NMR spectrum (CD_3CN, 250 MHz) of [(terpy)Ru(dpqtpy)Co(dpqtpy)Ru(terpy)][PF_6]$_6$

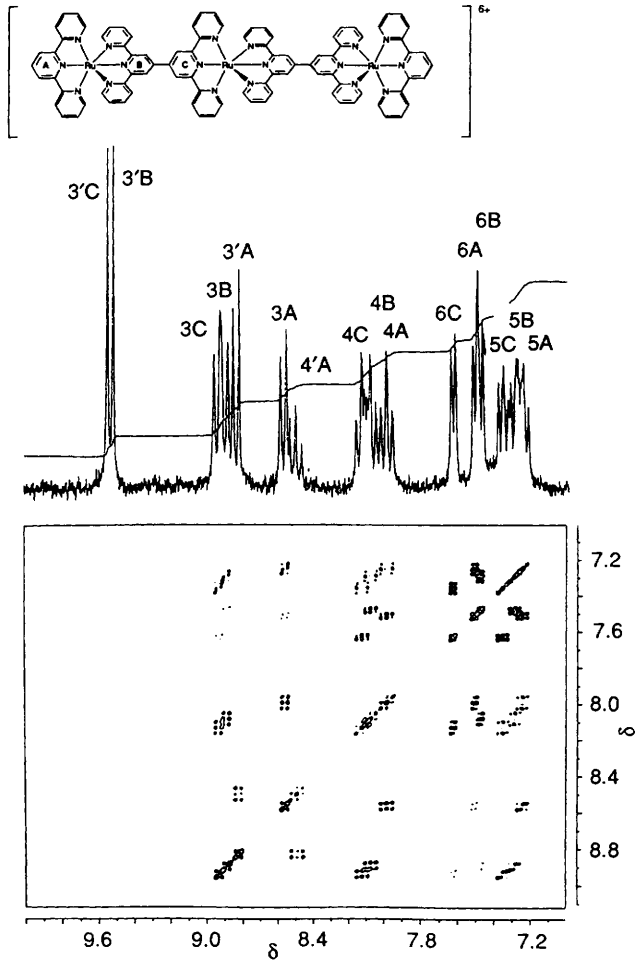

Fig. 5 Proton NMR and COSY spectra (CD_3CN, 250 MHz) of [(terpy)Ru(dpqtpy)Ru(dpqtpy)Ru(terpy)][PF_6]$_6$

and have been unambiguously assigned (Table 3) by a two-dimensional COSY experiment.

The heterotrinuclear complexes [(terpy)Ru(dpqtpy)Co^{II}-(dpqtpy)Ru(terpy)][PF_6]$_6$ and [(terpy)Ru(dpqtpy)Co^{III}-(dpqtpy)Ru(terpy)][PF_6]$_7$ are both electrochemically active (Table 4), and exhibit single reversible one-electron Ru^{II}–Ru^{III} processes at 0.96 and 0.94 V respectively. This compares very favourably with values of 0.96 V for [(terpy)Ru(dpqtpy)-Ru(terpy)][PF_6]$_4$ and 0.97 V for [(terpy)Ru(dpqtpy)Fe-(dpqtpy)Ru(terpy)][PF_6]$_6$, indicating that the nature of the central metal has little influence upon the redox behaviour of the adjacent ruthenium atoms. Three reversible reductive processes are also observed for [(terpy)Ru(dpqtpy)Co^{II}-(dpqtpy)Ru(terpy)][PF_6]$_6$, although these are only very poorly resolved in the cobalt(III) case. Rather surprisingly, we have not been able to observe a Co^{II}–Co^{III} process in the cyclic voltammetry of either [(terpy)Ru(dpqtpy)Co^{II}(dpqtpy)-Ru(terpy)][PF_6]$_6$ or [(terpy)Ru(dpqtpy)Co^{III}(dpqtpy)Ru-(terpy)][PF_6]$_7$. This is slightly surprising for [(terpy)-Ru(dpqtpy)Co^{II}(dpqtpy)Ru(terpy)][PF_6]$_6$, given that [Co-(terpy)$_2$][PF_6]$_2$ exhibits a reversible Co^{II}–Co^{III} process at −0.09 V.[23] We merely note that the Co^{II}–Co^{III} couple in a related heterotrinuclear complex [Co(fterpy)$_2$][PF_6] is observed as a poorly resolved process at −0.18 V.[24]

The trinuclear ruthenium complex [(terpy)Ru(dpqtpy)Ru-(dpqtpy)Ru(terpy)][PF_6]$_6$ is readily obtained by treating '$RuCl_3$·nH_2O' with 2 equivalents of the *ligand-complex* [Ru(terpy)(dpqtpy)][PF_6]$_2$ in hot ethane-1,2-diol. The pure homotrinuclear complex was obtained as a dark brown powder in 42% yield after recrystallisation. There was no necessity for a chromatographic purification. The partial elemental analysis (Table 1) remained poor, even after repeated recrystallisation and thorough drying. We have generally observed low carbon and nitrogen results from combustion analysis of polynuclear ruthenium complexes, and believe that the formation of ruthenium carbido and nitrido species leads to incomplete combustion. The FIB mass spectrum of the complex exhibits peaks showing a successive loss of hexafluorophosphate counter ions at *m/z* 2427, [P − PF_6]$^+$; 2281, [P − 2PF_6]$^+$; and 2135, [P − 3PF_6]$^+$. The ^{1}H NMR spectrum of a CD_3CN solution of the complex exhibits only 16 signals (Table 3) as expected given the symmetry about the central ruthenium. Comparisons with chemical shift data for [(terpy)Ru(dpqtpy)Ru(terpy)][PF_6]$_4$ and a two-dimensional COSY experiment were used to make the final assignments (Fig. 5). The chemical shifts are fully in accord with the patterns discussed earlier. The increase in charge upon passing from [(terpy)Ru(dpqtpy)Ru(terpy)]$^{4+}$ to [(terpy)Ru(dpqtpy)Ru-(dpqtpy)Ru(terpy)]$^{6+}$ does not cause any further downfield shifting of resonances. A single quasi-reversible oxidation process is observed at 0.98 V in the cyclic voltammogram of [(terpy)Ru(dpqtpy)Ru(dpqtpy)Ru(terpy)][PF_6]$_6$ (Table 4). Presumably the two different {RuN_6} environments are sufficiently similar that the two-electron Ru^{II}–Ru^{III} process of the two terminal ruthenium centres is coincident with the one-electron Ru^{II}–Ru^{III} couple of the central metal. Two ligand-centred reductive processes are resolved, with further ones being obscured by an absorption spike.

The electronic spectrum of [(terpy)Ru(dpqtpy)Ru(dpqtpy)Ru(terpy)][PF_6]$_6$ exhibits a broad, intense, m.l.c.t transition

at λ_{max} 525 nm (ε 82 800 dm^3 mol^{-1} cm^{-1}). This presumably corresponds to two separate superimposed m.l.c.t. transitions, from the two identical terminal ruthenium centres and from the other, central, ruthenium atom. It is of note that with increasing nuclearity the energy of the m.l.c.t. transition reduces. Mononuclear $[Ru(terpy)(dpqtpy)]^{2+}$ has λ_{max} 482 nm, dinuclear $[(terpy)Ru(dpqtpy)Ru(terpy)]^{4+}$ has λ_{max} 514 nm, whilst trinuclear $[(terpy)Ru(dpqtpy)Ru(dpqtpy)Ru(terpy)]^{6+}$ has λ_{max} 525 nm. The absorption coefficient of 82 800 dm^3 mol^{-1} cm^{-1} is of the magnitude expected for a trinuclear complex.

The availability of the *ligand-complex* allows the preparation of a range of other novel complexes. The mixed-metal ruthenium–osmium dinuclear species $[(terpy)Ru(dpqtpy)Os(terpy)]^{4+}$ can be prepared by treating equimolar quantities of $[Ru(terpy)(dpqtpy)][PF_6]_2$ with $[Os(terpy)Cl_3]$ in hot ethane-1,2-diol (Scheme 4). After chromatographic purification the purple salt $[(terpy)Ru(dpqtpy)Os(terpy)][PF_6]_4$ may be isolated. For spectroscopic comparison, the complexes $[(terpy)Os(dpqtpy)Os(terpy)][PF_6]_4$ and $[Os(terpy)_2][PF_6]_2$[25] were also prepared, the former by reaction of 2.2 equivalents of $[Os(terpy)Cl_3]$ with dpqtpy, and the latter by reaction of equimolar quantities of $[Os(terpy)Cl_3]$ and terpy, in both cases at reflux in ethane-1,2-diol. The complexes were isolated as hexafluorophosphate salts following chromatographic purification. In each case, elemental analysis and mass spectrometry (FAB or FIB) gave results consistent with these formulations. The ^1H NMR spectrum of a CD_3CN solution of $[Os(terpy)_2][PF_6]_2$ showed the expected six resonances (Table 3). The spectrum was assigned by inspection of the coupling patterns and comparison with the ^1H NMR spectrum of $[Ru(terpy)_2][PF_6]_2$. The dinuclear complex $[(terpy)Os(dpqtpy)Os(terpy)][PF_6]_4$ exhibits 11 resonances in its ^1H NMR spectrum, corresponding to the two different terpy domains, and a full assignment was made by a two-dimensional COSY experiment, and by comparison with the spectrum of $[Os(terpy)_2][PF_6]_2$. Finally, the heterodinuclear complex $[(terpy)Ru(dpqtpy)Os(terpy)][PF_6]_4$ exhibits 22 peaks in its ^1H NMR spectrum, assigned to a total of four different terpy domains. Assignments were made by a two-dimensional COSY experiment, and by comparison with chemical shift data for $[(terpy)Ru(dpqtpy)Ru(terpy)][PF_6]_4$ and $[(terpy)Os(dpqtpy)Os(terpy)][PF_6]_4$. To summarise these data, we may say that the osmium complexes closely resemble their ruthenium counterparts. For example, upon passing from $[Os(terpy)_2]^{2+}$ to $[(terpy)Os(dpqtpy)Os(terpy)]^{4+}$ there is a downfield shift of approximately δ 0.8. The chemical shifts of the terpy domains bonded to the ruthenium in $[(terpy)Ru(dpqtpy)Os(terpy)][PF_6]_4$ closely resemble those of $[(terpy)Ru(dpqtpy)Ru(terpy)][PF_6]_4$ whilst those co-ordinated to osmium resemble those in $[(terpy)Os(dpqtpy)Os(terpy)][PF_6]_4$.

Each of these osmium complexes is electrochemically active. The complex $[(terpy)Os(dpqtpy)Os(terpy)][PF_6]_4$ exhibits a reversible two-electron process at 0.62 V corresponding to the Os^{II}–Os^{III} process, as well as three ligand-centred reductions. The heterodinuclear complex $[(terpy)Ru(dpqtpy)Os(terpy)][PF_6]_4$ shows two one-electron processes at 0.59 and 0.95 V, corresponding to the Os^{II}–Os^{III} and the Ru^{II}–Ru^{III} couples respectively. These potentials are effectively identical to those observed for the homonuclear species $[(terpy)Os(dpqtpy)Os(terpy)][PF_6]_4$ and $[(terpy)Ru(dpqtpy)Ru(terpy)][PF_6]_4$, and it may be concluded that there is little interaction between the metal centres in the ground state. The heterodinuclear species also has two clearly resolved reductive processes, with further ones being obscured by an absorption spike. For comparison, the mononuclear complex $[Os(terpy)_2][PF_6]_2$ shows an Os^{II}–Os^{III} complex at 0.58 V and also undergoes two ligand-centred reductive processes.

Osmium terpy complexes generally exhibit similar electronic spectra to their ruthenium analogues.[10,26] The most prominent feature of the absorption spectrum of $[Os(terpy)_2][PF_6]_2$ in acetonitrile solution is an intense m.l.c.t. transition at λ_{max} 475 nm ε 15 400 dm^3 mol^{-1} cm^{-1}) {*cf.* λ_{max} 475 nm (ε 11 600 dm^3 mol^{-1} cm^{-1}) for $[Ru(terpy)_2][PF_6]_2$}.[27] An additional feature of the spectrum of the osmium complex is a second transition of lower intensity at lower energy, λ_{max} 656 nm (ε 4200 dm^3 mol^{-1} cm^{-1}). This is responsible for the difference in colour of the ruthenium and osmium complexes. The dinuclear complex $[(terpy)Os(dpqtpy)Os(terpy)][PF_6]_4$ exhibits its main m.l.c.t. transition at λ_{max} 519 nm (ε 43 800 dm^3 mol^{-1} cm^{-1}), a shift of 44 nm to lower energy compared to $[Os(terpy)_2][PF_6]_2$. This shift is virtually identical to that which occurs for the ruthenium analogue $[(terpy)Ru(dpqtpy)Ru(terpy)][PF_6]_4$ (λ_{max} 514 nm, ε 49 600 dm^3 mol^{-1} cm^{-1}). The second, less-intense m.l.c.t. band is also shifted to lower energy (λ_{max} 685 nm, ε 16 200 dm^3 mol^{-1} cm^{-1}) for the diosmium(II) complex. The heterodinuclear complex $[(terpy)Ru(dpqtpy)Os(terpy)][PF_6]_4$ exhibits two m.l.c.t. transitions at λ_{max} 515 (41 000) and λ 671 nm (ε 5800 dm^3 mol^{-1} cm^{-1}). The former can be assigned to absorptions of both the ruthenium and the osmium centres, and the absorption coefficient is compatible with this expectation. The second absorption is purely from the osmium, and this is confirmed by the small absorption coefficient.

We have, thus far, used our new *ligand-complexes* to prepare di- and tri-nuclear complexes. In ruthenium(II) homo-dinuclear and -trinuclear complexes the electronic interactions were such that it was not possible to observe two or more separate Ru^{II}–Ru^{III} processes; mixed-oxidation-state complexes did not seem to be particularly stabilised. We have also shown that in heteronuclear complexes an asymmetry may be introduced such that different metal centres (ruthenium–iron, –cobalt or –osmium) undergo redox processes at different potentials. In our final application of this methodology we will now demonstrate that it is possible to generate complexes which exhibit two or more Ru^{II}–Ru^{III} processes by the use of various X-terpy terminator ligands. Our general target was complexes of the type $[(X\text{-}terpy)Ru(dpqtpy)Ru(Y\text{-}terpy)]^{4+}$ We illustrate here the preparation of complexes containing representative electron-releasing and -withdrawing substituents, and show that extremes of behaviour may be achieved by the use of both strongly electron-withdrawing and strongly electron-accepting ligands in the same dinuclear complex.

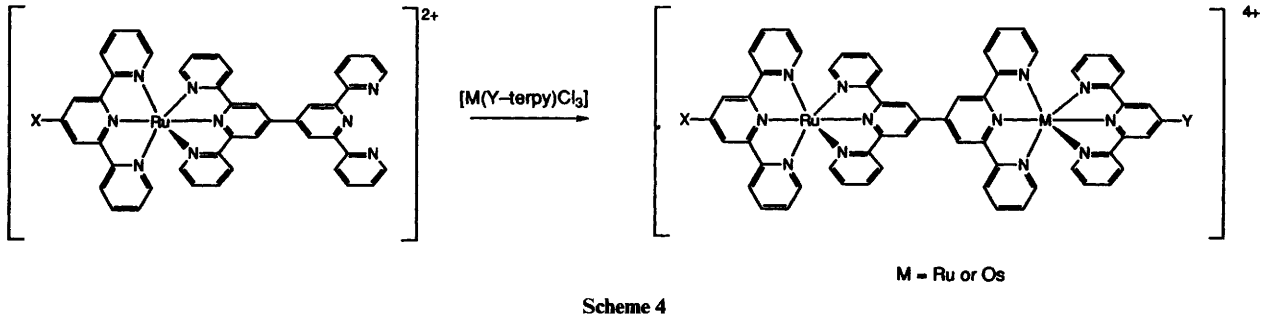

Scheme 4

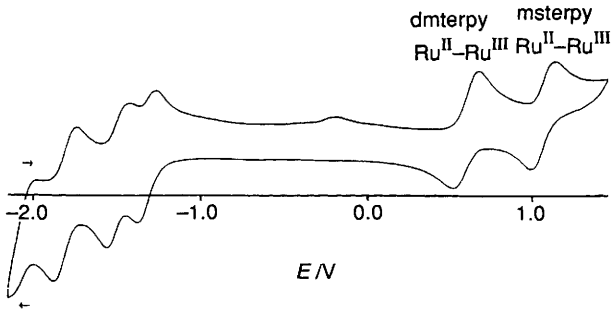

Fig. 6 Cyclic voltammogram (potentials *vs.* internal ferrocene–ferrocenium) of an acetonitrile solution of [(dmterpy)Ru(dpqtpy)-Ru(msterpy)][PF_6]$_4$

The *ligand-complex* [Ru(terpy)(dpqtpy)][PF_6]$_2$ reacts smoothly with an equimolar quantity of [Ru(dmterpy)Cl_3] in hot ethane-1,2-diol to give [(terpy)Ru(dpqtpy)Ru(dmterpy)]$^{4+}$; after chromatographic work-up [(terpy)Ru(dpqtpy)Ru(dmterpy)][PF_6]$_4$ was obtained as a red-brown solid (35% yield). Prolonged reaction times should be avoided as ligand scrambling can occur, to give the complexes [(dmterpy)Ru(dpqtpy)Ru(dmterpy)]$^{4+}$ and [(terpy)Ru(dpqtpy)-Ru(terpy)]$^{4+}$. In a similar reaction [Ru(terpy)(dpqtpy)][PF_6]$_2$ reacts smoothly with an equimolar quantity of [Ru(msterpy)-Cl_3] in methanol containing a few drops of *N*-ethylmorpholine to give [(terpy)Ru(dpqtpy)Ru(msterpy)][PF_6]$_4$ as a red solid (35%). Finally, the complex [(msterpy)Ru(dpqtpy)Ru-(dmterpy)][PF_6]$_4$ was obtained as a red-brown solid (21%) from the reaction of [Ru(msterpy)(dpqtpy)][PF_6]$_2$ with an equimolar quantity of [Ru(dmterpy)Cl_3] in methanol containing a few drops of *N*-ethylmorpholine.

The complexes were obtained in acceptable yield and elemental analysis (Table 1) and mass spectrometry (FAB and FIB) are consistent with the proposed formulations. The ^{1}H NMR spectrum a CD_3CN solution of each complex exhibits 20–22 peaks (Table 3), as a result of the four different types of terpy domain which are present. Assignments were made by two-dimensional COSY experiments, and by comparison with chemical shift data for the corresponding complexes [(X-terpy)Ru(dpqtpy)Ru(X-terpy)][PF_6]$_4$ and [(Y-terpy)Ru-(dpqtpy)Ru(Y-terpy)][PF_6]$_4$. Chemical shifts are as expected, indicating that there is little transmission of electronic information from one terminator *ligand* to the other.

All three [(X-terpy)Ru(dpqtpy)Ru(Y-terpy)][PF_6]$_4$ complexes studied are electrochemically active, and each exhibits two quasi-reversible Ru^{II}–Ru^{III} processes (Table 4). Up to four reversible ligand-centred reductive processes are also observed, though in some cases these are partially obscured by an absorption spike. As expected from our discussion earlier, the two Ru^{II}–Ru^{III} potentials for each complex [(X-terpy)-Ru(dpqtpy)Ru(Y-terpy)][PF_6]$_4$ are identical to those for the appropriate environments in [(X-terpy)Ru(dpqtpy)Ru(X-terpy)][PF_6]$_4$ and [(Y-terpy)Ru(dpqtpy)Ru(Y-terpy)][PF_6]$_4$ (Fig. 6). The electronic spectra of the three complexes (Table 5) are, however, more interesting. The low-energy m.l.c.t. transition of [(X-terpy)Ru(dpqtpy)Ru(Y-terpy)][PF_6]$_4$ appears at a wavelength (λ_{max}) which is very similar to the average wavelength of the two parent complexes [(X-terpy)Ru-(dpqtpy)Ru(X-terpy)][PF_6]$_4$ and [(Y-terpy)Ru(dpqtpy)-Ru(Y-terpy)][PF_6]$_4$.

In conclusion, we have developed a new building block for the preparation of a range of novel metallosupramolecular oligomers. These reactions are summarised in the Schemes. A range of hetero- and homo-metallic di- and tri-nuclear complexes have been prepared. We are therefore currently investigating the photochemical and photophysical properties of mixed-ligand dinuclear complexes incorporating an electron-donating ligand at one end and an electron-acceptor ligand at the other, an arrangement which is ideally suited to electron or energy transfer.

Acknowledgements

We thank the Schweizerischer Nationalfonds zur Förderung der wissenschaftlichen Forschung (Grant number: 21-37325.93) and the SERC (UK) for support, Johnson Matthey for the loan of precious metals, and Professors J.-P. Sauvage and V. Balzani for helpful discussions.

References

1 E. C. Constable, A. M. W. Cargill Thompson and D. A. Tocher in, *Supramolecular Chemistry*, eds. V. Balzani and L. De Cola, Klewer Academic Press, Dordrech, 1992, p. 219.
2 E. C. Constable, *Chem. Ind. (London)*, 1994, 56.
3 E. C. Constable, *Prog. Inorg. Chem.*, 1994, **42**, 67.
4 G. Denti, S. Serroni, S. Campagna, A. Juris, M. Ciano and V. Balzani, in *Perspectives in Coordination Chemistry*, eds. A. F. Williams, C. Floriani and A. E. Merbach, VCH, Weinheim, 1992, p.153.
5 V. Balzani and F. Scandola, *Supramolecular Photochemistry*, Ellis Horwood, Chichester, 1991; G. J. Karvanos, *Photoinduced Electron Transfer*, VCH and VHCA, Weinheim and Basel, 1992, p. 153.
6 E. C. Constable in, *Transition Metals in Supramolecular Chemistry*, eds. L. Fabbrizzi and A. Poggi, Klewer Academic Press, Dordrecht, 1994, p. 81; E. C. Constable, *Makromol. Symp.*, 1994, **77**, 219.
7 E. C. Constable and A. M. W. Cargill Thompson, *J. Chem. Soc., Dalton Trans.*, 1992, 2947.
8 E. C. Constable and M. D. Ward, *J. Chem. Soc., Dalton Trans.*, 1990, 1405; E. C. Constable and A. M. W. Cargill Thompson, *J. Chem. Soc., Dalton Trans.*, 1992, 3467; E. C. Constable, A. M. W. Cargill Thompson and D. A. Tocher, *Supramol. Chem.*, 1993, **3**, 9.
9 E. C. Constable and A. M. W. Cargill Thompson, *J. Chem. Soc., Chem. Commun.*, 1992, 617; *J. Chem. Soc., Dalton Trans.*, 1994, 1409; G. R. Newkome, F. Cardullo, E. C. Constable, C. N. Moorefield and A. M. W. Cargill Thompson, *J. Chem. Soc., Chem. Commun.*, 1993, 925.
10 F. Barigelletti, L. Flamigni, V. Balzani, J.-P. Collin, J.-P. Sauvage, A. Sour, E. C. Constable and A. M. W. Cargill Thompson, *J. Chem. Soc., Chem. Commun.*, 1993, 942; *Coord. Chem. Rev.*, 1994, **132**, 209; *J. Am. Chem. Soc.*, 1994, **116**, 7692.
11 S. Serroni, G. Denti, S. Campagna, A. Juris, M. Ciano and V. Balzani, *Angew. Chem., Int. Ed. Engl.*, 1992, **31**, 1493.
12 E. C. Constable, A. M. W. Cargill Thompson and D. A. Tocher, *Polymer Preprints*, 1993, **34**, 110; *Makromol. Symp.*, 1994, **77**, 219.
13 D. L. Jameson and L. E. Guise, *Tetrahedron Lett.*, 1991, **32**, 1999.
14 E. C. Constable, A. M. W. Cargill Thompson and D. A. Tocher, *New J. Chem.*, 1992, **16**, 855; E. C. Constable in *Inorganic Experiments*, ed. J. D. Woollins, VCH, Weinheim, 1994, p. 189.
15 N. Armaroli, V. Balzani, E. C. Constable, M. Maestri and A. M. W. Cargill Thompson, *Polyhedron*, 1992, **11**, 2707.
16 R. P. Thummel and S. Chirayil, *Inorg. Chim. Acta*, 1988, **154**, 77.
17 V. Grosshenny and R. Ziessel, *J Organomet. Chem.*, 1993, **453**, C19.
18 M. Beley, S. Chodorowski, J. P. Collin, J. P. Sauvage, L. Flamigni and F. Barigelletti, *Inorg. Chem.*, 1994, **33**, 2543; J. P. Sauvage, J. P. Collin, J. C. Chambron, S. Guillerez, C. Coudret, V. Balzani, F. Barigelletti, L. Decola and L. Flamigni, *Chem. Rev.*, 1994, **94**, 993.
19 E. C. Constable, *Inorg. Chim. Acta*, 1984, **82**, 53; E. C. Constable and T. A. Leese, *Inorg. Chim. Acta*, 1988, **146**, 55.
20 M. Maestri, N. Armaroli, V. Balzani, E. C. Constable and A. M. W. Cargill Thompson, *Inorg. Chem.*, in the press.
21 E. C. Constable, J. V. Walker and D. A. Tocher, *J. Chem. Soc., Chem. Commun.*, 1992, 768; E. C. Constable and J. V. Walker, *J. Chem. Soc., Chem. Commun.*, 1992, 884; E. C. Constable, M. A. M. Daniels, M. G. B. Drew, D. A. Tocher, J. V. Walker and P. D. Wood, *J. Chem. Soc., Dalton Trans.*, 1993, 1947; E. C. Constable, A. J. Edwards, P. R. Raithby and J. V. Walker, *Angew. Chem., Int. Ed. Engl.*, 1993, **32**, 1465; E. C. Constable, R. Martínez-Máñez, A. M. W. Cargill Thompson and J. V. Walker, *J. Chem. Soc., Dalton Trans.*, 1994, 1585.

22 E. C. Constable and D. Phillips, unpublished work.
23 E. C. Constable, *Adv. Inorg. Chem. Radiochem.*, 1987, **30**, 69.
24 E. C. Constable, A. J. Edwards, R. Martínez-Máñez, P. R. Raithby and A. M. W. Cargill Thompson, *J. Chem. Soc., Dalton Trans.*, 1994, 645.
25 E. C. Constable, P. R. Raithby and D. N. Smit, *Polyhedron*, 1989, **8**, 367.
26 B. J. Pankuch, D. E. Lacky and G. A. Crosby, *J. Phys. Chem.*, 1980, **84**, 2061.
27 A. Juris, V. Balzani, F. Barigelletti, S. Campagna, P. Belser and A. von Zelewsky, *Coord. Chem. Rev.*, 1988, **84**, 85.

Received 29*th November* 1994; *Paper* 4/07272C